PAPER • OPEN ACCESS

High-temperature mechanical properties of cast Al–Si–Cu–Mg alloy by combined additions of cerium and zirconium

IOP ebooks™

Bringing you innovative digital publishing with leading voices to create your essential collection of books in STEM research.

Start exploring the collection - download the first chapter of every title for free.

Materials Research Express

PAPER

High-temperature mechanical properties of cast Al–Si–Cu–Mg alloy by combined additions of cerium and zirconium

William Lemos Bevilaqua ⓘ , Antonio Ricardo Stadtlander, Andre Ronaldo Froehlich, Guilherme Vieira Braga Lemos and Afonso Reguly ⓘ

Post-graduation Program in Mining, Metallurgical and Materials Engineering (PPGE3M), Federal University of Rio Grande do Sul (UFRGS), Av. Bento Gonçalves, 9500. Porto Alegre, CEP 91501-970, Brazil

E-mail: bevilaquawilliam@gmail.com

Abstract

The main aim of this work is to investigate the effects of combinative Ce and Zr additions (0.3 wt% Ce + 0.16 wt% Zr; 0.3 wt% Ce + 0.27 wt% Zr and 0.3 wt% Ce + 0.36 wt% Zr) on the microstructure and mechanical properties in cast Al–Si–Cu–Mg alloy. The microstructures features were investigated by optical microscope, scanning electron microscope and hardness measurements. The microstructural analysis has shown that the increase of Ce and Zr contents increases the volume fraction of intermetallics formed during the solidification leading to grain refinement and changes in silicon morphology of the as-cast microstructure. The intermetallics formed do not dissolve during the solution heating treatment (T6). The mechanical behavior at room and high temperatures (175, 210, 245 and 275 °C) was determined from uniaxial tensile tests. The high thermal stability of Al–Si–Cu–La–Ce and Al–Si–Zr–Ti–Mg phases found in microstructure, in particular for the alloy containing 0.3 wt% Ce + 0.27 wt% Zr, is responsible for the increase to 6.7% and 5.1% the ultimate strength at 210 °C and 275 °C respectively, compared with the standard alloy.

1. Introduction

The increasing requirement to improve fuel economy triggered by concerns about global warming and energy usage has a significant influence on the choice of materials [1], leading to the need for lighter alloys accompanied with enhanced mechanical properties [2]. For example, modern internal combustion engines require relatively high temperatures operations, usually above 250 °C, and pressures up to 180 bar to reach demands of fuel consumption and standards [3]. However, it is well known that cast aluminum alloys have operational limitations when used at temperatures up to 150 °C due to the recognizable low thermal stability of Al_2Cu and Mg_2Si precipitates. In this context, it is clear that the main challenge for aluminum alloys is to keep their strength at temperatures above 200 °C [4, 5].

In order to improve the mechanical properties of aluminum alloys, strategies involving minor additions of transition metals like zirconium [6], rare-earth metals, such as cerium [7–9], lithium [10], Al_3O_2 nanocomposites [11] and Al-Mg_2Si *in situ* composites [12] can be cited. In recent years, efforts have been made for improving cast alloys mechanical properties, mainly in superior temperatures than the ones of the conventional applications. A significant number of studies on cast Al–Si–Cu–Mg alloys [13–18] were conducted due to its important applications in the transport sector in a large variety of components. Basically, in order to improve the strength, particularly at high temperatures, alloying elements that exhibit both limited solid solubility and low diffusivity in Al must be added [19]. Recent studies on aluminum alloys modified with the minor Zr additions [3, 5, 16, 20–22] demonstrated a significant enhancement in high-temperature mechanical properties due to the increase of volume fraction of high-stable intermetallic phases formed in the microstructure.

Apart from Zr additions in aluminum alloys, minor additions of rare-earth in aluminum alloys have been attracted significant attention, especially cerium additions in the range of 0.1 to 0.3 wt%. It was reported that in Al–Zn–Mg–Cu cast alloy, Ce addition results in refinement of the cast dendritic structure [23], and modifies the eutectic silicon

Table 1. Chemical composition (wt%) of standard and modified Al–Si–Cu–Mg alloys.

Alloy Code	Si	Fe	Cu	Mn	Mg	Zn	Ti	Ce	Zr
C1	8.99	0.13	1.90	0.003	0.45	0.0016	0.11	—	—
C2	8.92	0.15	1.87	0.006	0.45	0.07	0.12	0.34	0.16
C3	8.95	0.16	1.90	0.011	0.44	0.11	0.12	0.31	0.27
C4	8.84	0.19	1.90	0.013	0.44	0.15	0.12	0.30	0.36

morphology [24]. Additionally, Ce interacts with Al_2Cu precipitates producing changes in morphology and precipitation hardening behavior [25]. Additionally, extensive studies [26, 27] in 2519A aluminum alloy plate show that Ce leads to an increased precipitation phase volume fraction, as well as a more dispersive and homogeneous distribution promotes the precipitation of denser and finer θ' precipitates, which improves the tensile strength of the alloy at both room and elevated temperatures. Recently, [28] shows that cerium intermetallic phases are highly stable in Al–12Ce–4Si–0.4Mg (wt%), displaying a room temperature ultimate tensile strength of 400 MPa and yield strength of 320 MPa, with 80% mechanical property retention at 240 °C.

Although both Ce and Zr elements have been recognized over the past few years as potential alloying elements for some Al alloys, it should be remarked that combinative Ce and Zr additions in cast alloys, particularly in Al–Si–Cu–Mg alloys is a topic which has not been addressed in the literature. Therefore, the aim of this work is to investigate the effects of combined Ce and Zr additions on microstructure and high-temperature mechanical properties of the Al–Si–Cu–Mg cast alloy.

2. Experimental

2.1. Alloys and casting process

Modified Al–Si–Cu–Mg alloys were prepared with both minor Cerium (mischmetal 70%), and Zirconium (AlZr10%) master alloys. The alloys were produced in a 7 kg capacity graphite crucible, using an electrical resistance furnace, which was maintained at approximately 860 °C. The melt was degassed by pure argon, and poured into a permanent mold preheated by oxyacetylene neutral flame during 5 min The chemical composition of the alloys measured by optical emission spectroscopy technique is given in table 1.

After the casting process, samples were solubilized at 525 °C for 12 h, followed by quenching in warm water (65 °C) and then artificially aged at 180 °C for 8 h. The heat treatment parameters were selected according to the best results from previous experiments in order to optimize the alloy hardness.

2.2. Microstructural characterization

Macrographs of the longitudinal cross-section of ingots were prepared and the surface etched by concentrated Keller´s solution (5 ml Hydrofluoric acid + 10 ml Hydrochloric acid + 15 ml Nitric acid + 70 ml distilled water) according to the procedure described in [29]. Metallographic samples were prepared by standard procedures and etched with Keller´s reagent (5 ml Nitric acid, 3 ml Hydrochloric acid, 2 ml Hydrofluoric acid and 190 ml distilled water). The microstructure was observed by optical microscopy (Olympus-BX51M) and Scanning electron microscope (SEM-Shimadzu SSX-550 Superscan) equipped with energy dispersive x-ray spectroscopy detector (EDS).

Brinell hardness test was conducted according to ASTM E10 with 62.5 kg of load and a 2.5 mm diameter ball. Microhardness measurements of the α-aluminum matrix were carried out according to ASTM E384 with 25 g of load during 10 s. Both Brinell and Vickers hardness values are described by mean and standard deviation considering fifteen measurements.

2.3. Mechanical properties

Mechanical properties were evaluated in the MTS 810 machine test. The specimens were prepared as per ASTM E8 standard. The ultimate tensile strength (UTS) was recorded by the acquisition system of the machine test and the yield strength (YS) were obtained according to 0.2% offset strain. In addition, the high-temperature tensile tests were carried out according to ASTM E21, using a resistive heating furnace installed on the testing machine. In order to stabilize the temperature of interest, the specimens were maintained at a predetermined temperature for 30 min. The samples were tested at 20, 175, 210, 245 and 275 °C with a constant displacement rate of 0.005 mm s^{-1}. The fracture surfaces were later analyzed by SEM using the secondary electron (SE) mode.
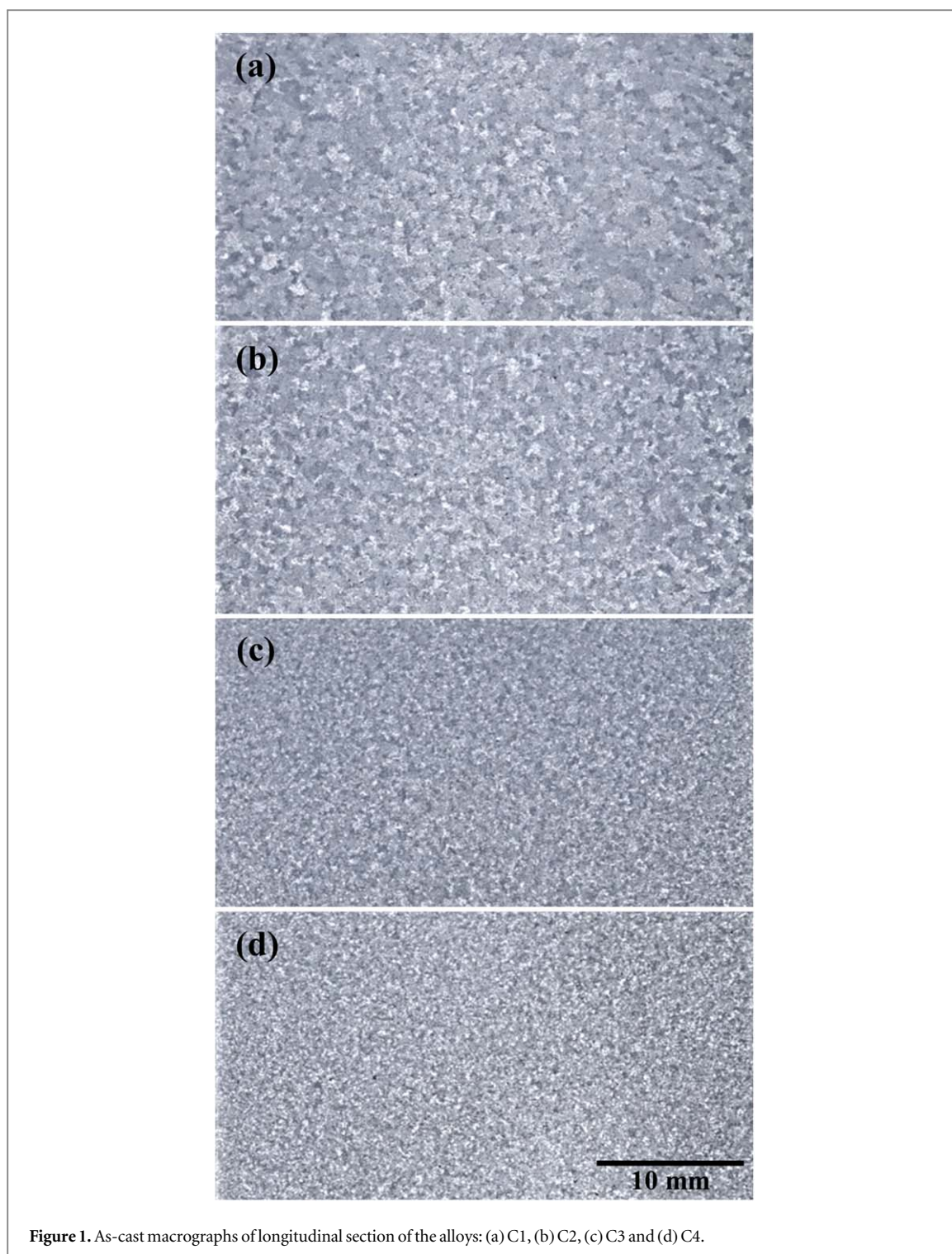
Figure 1. As-cast macrographs of longitudinal section of the alloys: (a) C1, (b) C2, (c) C3 and (d) C4.

3. Results and discussions

3.1. Microstructure and hardness

Figure 1 shows the standard macrostructure of the Al–Si–Cu–Mg ingots compared with Ce–Zr modified alloys. It is interesting to notice that the increment in Zr content ratio promotes a considerable refinement in the macrostructure (up to 0.27 wt%). Further Zr additions (0.36 wt%) do not strongly influence the macrostructure refinement which is a good agreement with the optimal 0.3 wt% Zr content also found by others [30, 31]. The grain refinement due to zirconium in cast alloys can be explained by the reaction $L + Al_3Zr = \alpha(Al)$ according to [32]. The Al_3Zr particles were acting as potential nucleation sites for the aluminum grain grown, suppressing the formation of columnar grains, as expected for cast alloys.

Figure 2. Light optical micrographs of alloys C1, C2, C3 and C4 respectively in ((a)–(d)—as-cast condition) and ((e)–(h)—T6 temper).
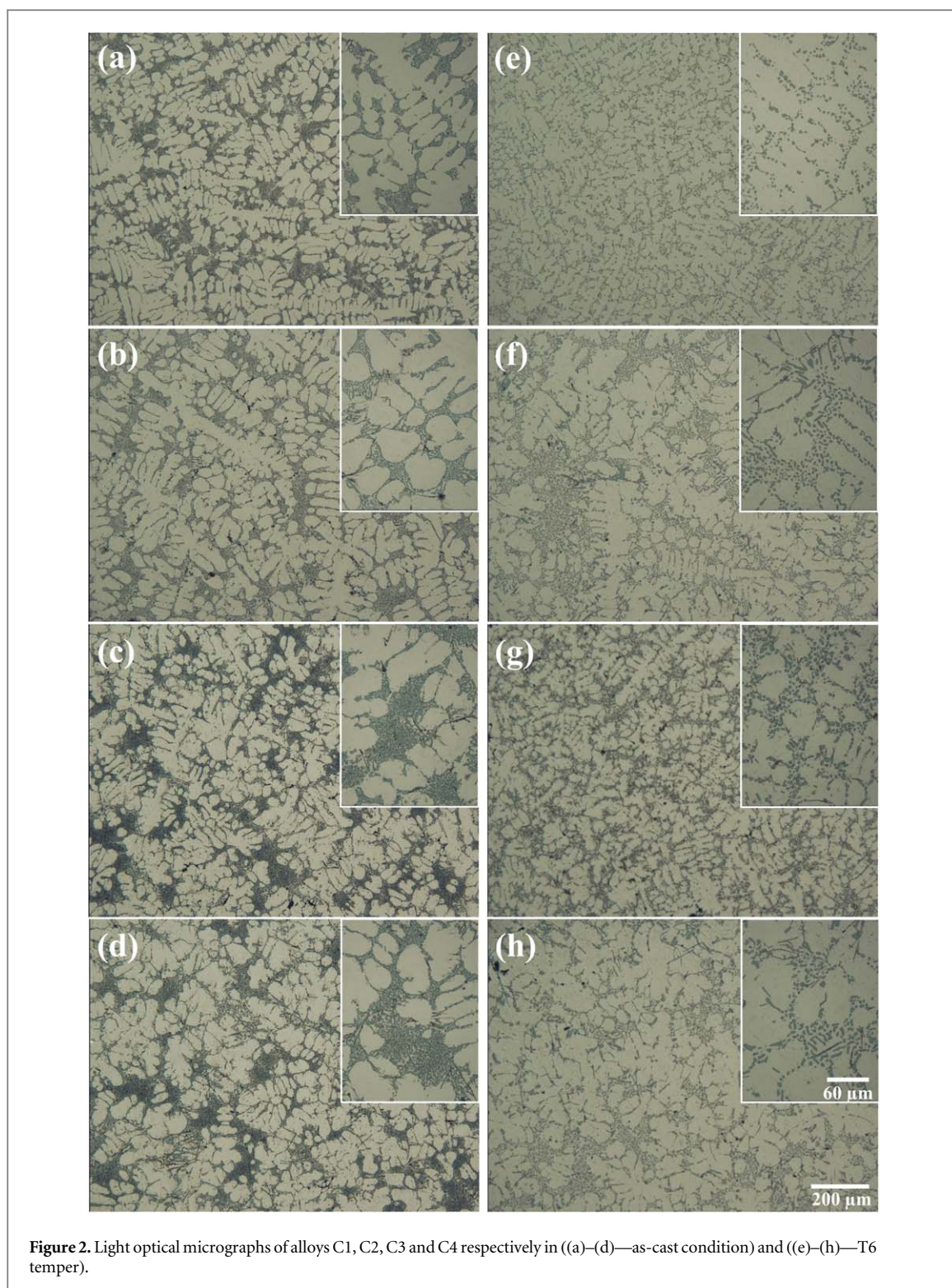
Figure 2 shows the microstructures of standard and modified alloys in the as-cast and T6 conditions. The as-cast microstructure is formed by α-aluminum dendritic network with eutectic silicon particles segregated into the interdendritic region. It can be observed that the simultaneous addition (Ce + Zr) changes the distribution of dendritic network leading to coarse silicon. According to cerium [33] and zirconium [34] binary phase diagram, their maximum solid solubility is 0.05 wt% and 0.083 wt%, respectively. This low solubility probably leads to a coarse network due to rejection of Ce and Zr to the interdendritic regions during solidification. After a solution heat treatment at 525 °C for 12 h, quenching and subsequent aging at 180 °C for 8 h, it may be noted that a fine eutectic silicon forms in standard alloys (C1). However, for the modified alloys (C2, C3, and C4), the silicon network did not fragment during ongoing of solution heating treatment.
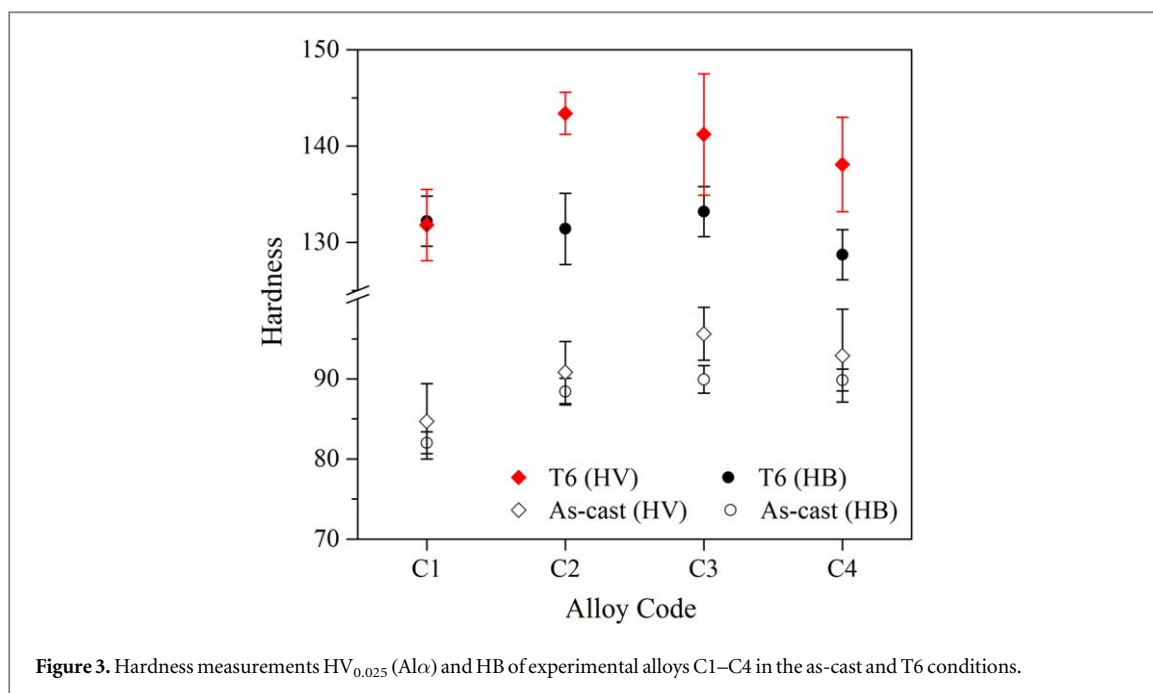
Figure 3. Hardness measurements $HV_{0.025}$ (Alα) and HB of experimental alloys C1–C4 in the as-cast and T6 conditions.

In [35], it was explained that during solution treatment, the Si eutectic undergoes the following transformations: fragmentation, spheroidization, and growth. The dominant phenomenon at any given time depends on the treatment temperature and the size and morphology of the original particles. Considering what was mentioned before, it could be inferred that the Ce and Zr addition affects these. The introduction of Ce–Zr elements modifies the eutectic silicon morphology during the solidification process, leading to different initial morphologies in each alloy possible affecting the stages of silicon particles fragmentation during solution treatment.

Figure 3 presents Brinell and Vickers measurements for C1, C2, C3, and C4 alloys in as-cast and T6 conditions. As expected, the precipitation hardening mechanism promoted a hardness enhancement in the T6 condition, and the Ce–Zr additions slightly increase the overall hardness of modified alloys. It is interesting to notice that alloys modified by Ce–Zr present a substantially increased microhardness value of α–aluminum (Alα) in the T6 condition. A possible explanation is that Zr precipitated as Al$_3$Zr particles during sufficiently long solutionizing treatments [36]. These particles can increase hardness, but do not have any significant influence on in the age-hardened process [31, 36].
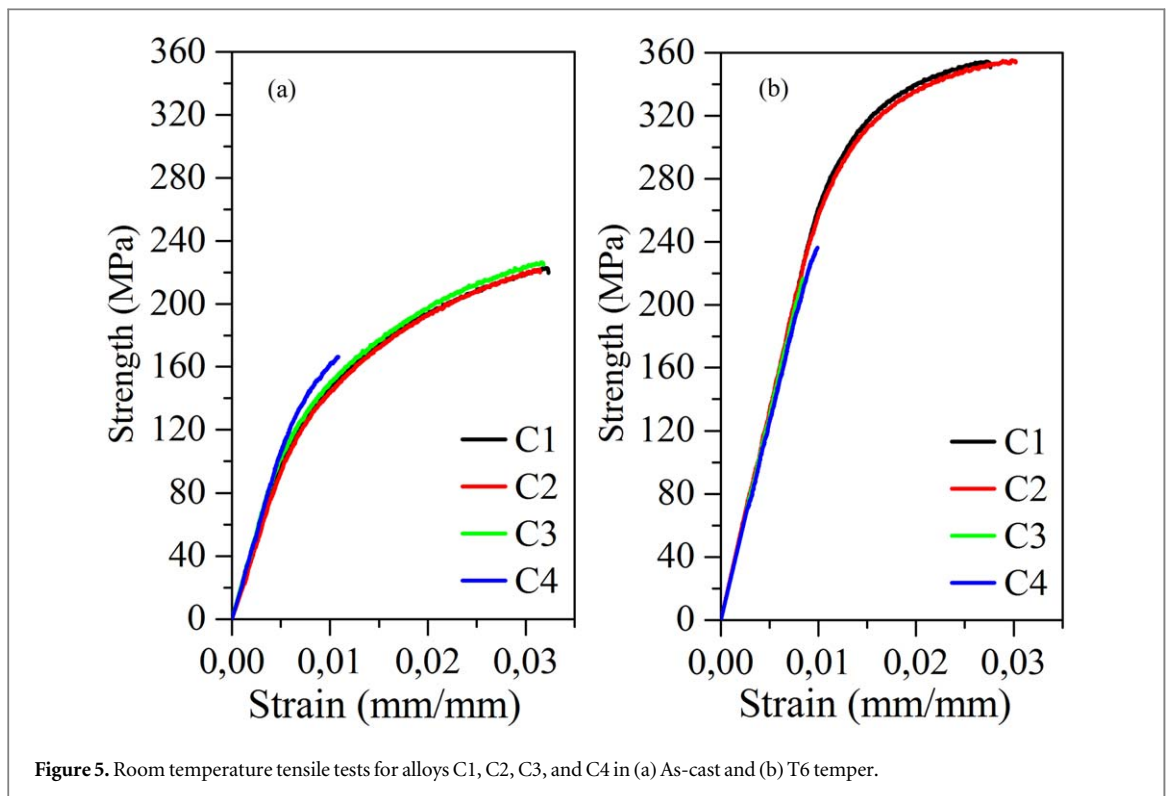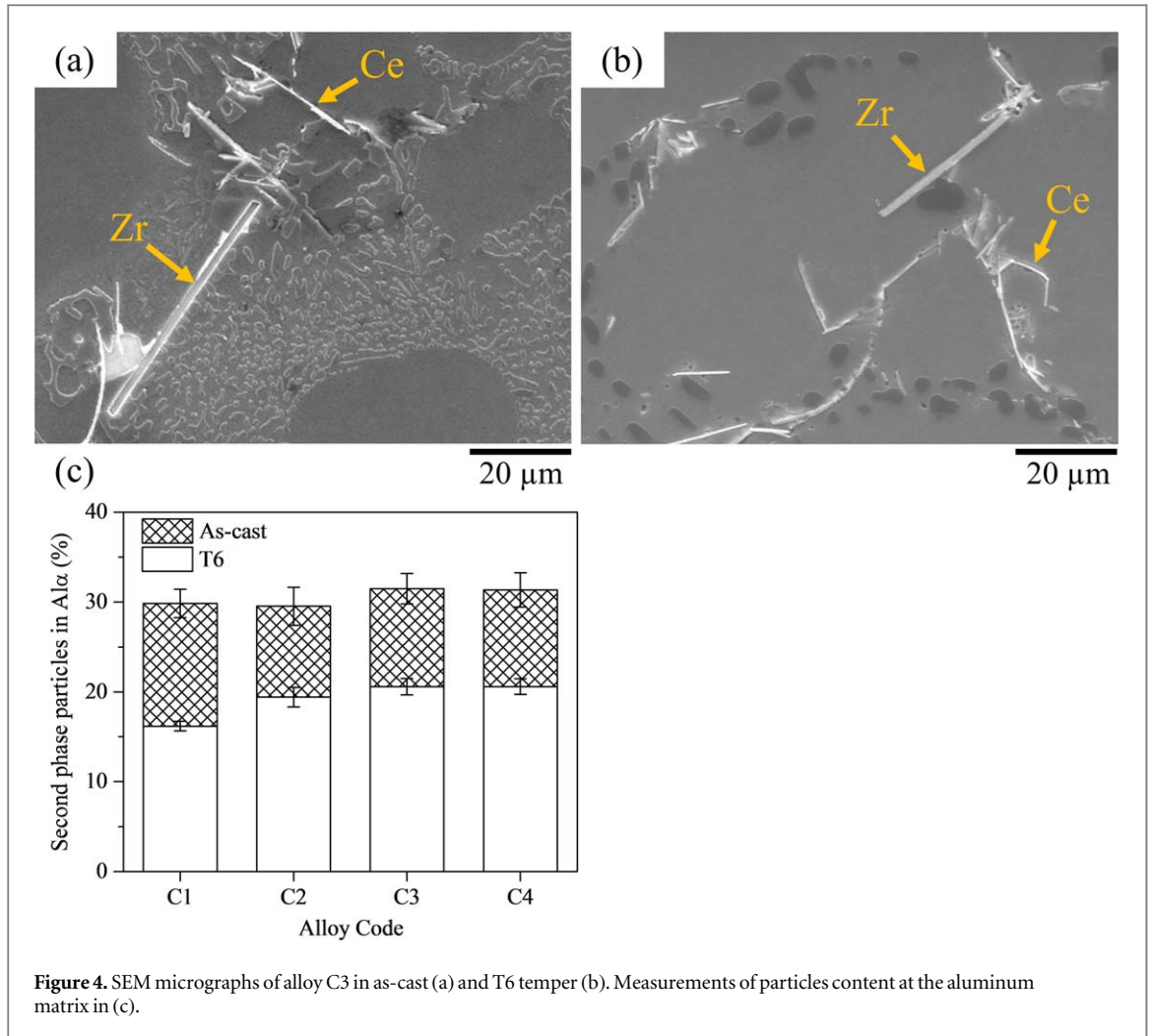
Another point of view is that Ce atoms enter in the Al matrix and cause the crystal lattices distortion and raise system energy, producing more vacancies aggregating around Ce promoting the precipitation of dense and finer θ' phase [26]. Therefore, the improvement in hardness of Alα might be related to residual Al$_3$Zr particles from solution heating treatment and the influence of cerium in age hardening. However, further transmission electron microscope investigations shall be carried out to clarify this.
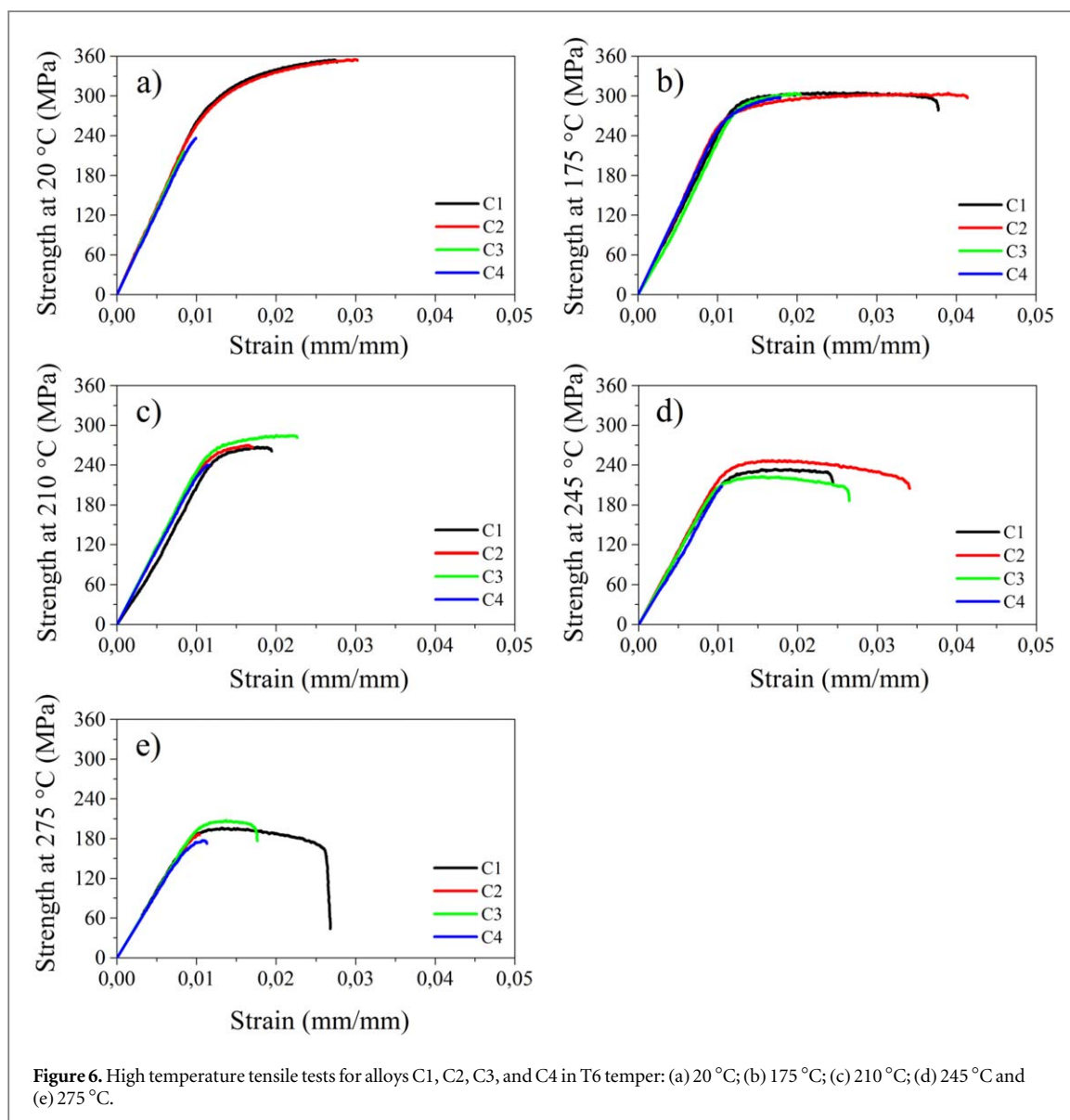
Figure 4 shows the microstructure of the C3 alloy where different intermetallic phases are observed in as-cast (figure 4(a)) and age-hardening conditions (figure 4(b)). Due to the low solubility of Ce and Zr in the Al matrix, during the solidification process, new intermetallic phases are formed and rejected to the interdendritic regions. It was identified by EDS analysis that Cerium combines with Al, Cu, and Si while Zirconium reacts with Al, Si, Mg, and Ti. Besides, no shreds of evidence from EDS analysis indicated phases with Ce–Zr. It is interesting to notice that coarse intermetallic phases formed by Ce and Zr remain undissolved in the matrix and do not change their shape after solution heating treatment at 525 °C by 12 h. This behavior was identified for all modified alloys (C2, C3 and C4), indicating that Ce and Zr intermetallic phases are highly stable in microstructure at high temperatures [26], and are not solutionized during solution treatment [37].

As can be seen in figure 4(c), the results from the measurements of the particles in the Al matrix before and after the solution heating treatment are reported. The modified alloys (C2, C3, and C4) remains with a major percentage of particles, leading to a conclusion that increasing the Zr content enhances the intermetallic phases undissolved in the matrix.

3.2. Mechanical properties

Figure 5 displays the ultimate tensile strength (UTS) as a function of strain for C1, C2, C3, and C4 alloys at 20 °C. For as-cast condition (figure 5(a)), no significant differences in UTS were observed between the standard and

Figure 4. SEM micrographs of alloy C3 in as-cast (a) and T6 temper (b). Measurements of particles content at the aluminum matrix in (c).

Figure 5. Room temperature tensile tests for alloys C1, C2, C3, and C4 in (a) As-cast and (b) T6 temper.

Figure 6. High temperature tensile tests for alloys C1, C2, C3, and C4 in T6 temper: (a) 20 °C; (b) 175 °C; (c) 210 °C; (d) 245 °C and (e) 275 °C.

modified alloys. Although, a substantial decrease in mechanical properties can be noticed for C4 alloy, which is probably related to the relatively high amount of intermetallic phases undissolved in the matrix (figure 4(c)). Considering the test carried out in the T6 condition (figure 5(b)), an increase in the mechanical properties due to the precipitation hardening of the aluminum matrix can be noted. The substantial decreasing in both UTS and strain of C3 (0.3 wt% Ce + 0.27 wt% Zr) and C4 (0.3 wt%Ce + 0.36 wt% Zr) alloys, which was not seen in the cast condition, is due to an increase in stress concentration factor around the Ce–Zr intermetallic phases due to the age hardening. Similar levels of mechanical properties achieved between C1 (standard alloy) and C2 (0.3 wt% Ce + 0.16 wt% Zr) alloys leads to the conclusion that additions of Ce–Zr in this range has not deleterious effects in mechanical behavior at room temperature.

Figure 6 shows the high-temperature mechanical properties of the C1, C2, C3, and C4 alloys in the T6 condition for different test temperatures. In general, an increase in temperature test produces a decrease in the UTS as well as an enhancement in strain. This behavior is well known and represents the effects of temperature over softening of the matrix, reduce of strengthening precipitates, and consequently, lower efficiency in hindering dislocations movement [18].

In figures 6(a) and (b), the tests undertaken at 20 °C and 175 °C respectively showed that C3 and C4 alloys present low ductility until the fracture. This behavior can be explained due to the excess of intermetallic phases in the Al matrix. However, considering the test temperatures of 210 °C (figure 6(c)), 245 °C (figure 6(d)) and 275 °C (figure 6(e)), the C2 and C3 alloys showed superior mechanical properties when compared with the standard alloy. In the test performed at 210 °C (figure 6(c)), the C3 alloy shows an increase of approximately 6.7% of UTS in comparison with C1 alloy. In addition, it can also be observed a superior performance of C2 alloy (> 5%) at 245 °C (figure 6(d)), and C3 alloy (> 5.6%) at 275 °C, in contrast to the standard alloy (C1). Still, the

Table 2. Mechanical properties of Ce–Zr modified Al–Si–Cu–Mg alloy in the T6 condition used in this work in comparison with another studies.

Alloy[a]	Test temperature (°C)	Yield strength (MPa)[b]	Ultimate tensile strength (MPa)
Al–Si–Cu–Mg modified with 0.3 wt% Ce + 0.27 wt% Zr (Present work)	25	299	354
	175	297	304
	210	269	284
	245	217	223
	275	204	207
354.0 modified with 0.21 wt% Ni + 0.19 wt% Zr [38]	25	317	348
	190	265	288
	250	—	228
	300	123	141
Al–7Si–1Cu–0.5Mg (wt) modified with 0.11 wt% Ti + 0.20 wt% Zr + 0.25 wt% V [39]	25	309	335
A356 modified with (Al$_2$O$_3$ 5 wt%—60 nm) [11]	25	248	292
	200	190	213
	250	125	148
	300	58	62

[a] Permanent mold casting.

[b] 0.2% offset strain.

behavior of plastic deformation reached until the fracture is predominant for the standard alloy, demonstrating that additions Ce and Zr intermetallics have a substantial effect in ductility, even at high temperatures.

More significant mechanical properties at high temperature due to Zr addition in cast Al–Si have been reported elsewhere [5, 20, 38]. Different behaviors detected in alloys C2 and C3 alloys might be related to the interaction of intermetallic phases with the Al matrix during the deformation process. Furthermore, the contribution of a nano-particle of Al$_8$Cu$_4$Ce [26], which was not investigated in this work, may have an essential impact on mechanical properties, especially at high temperature.
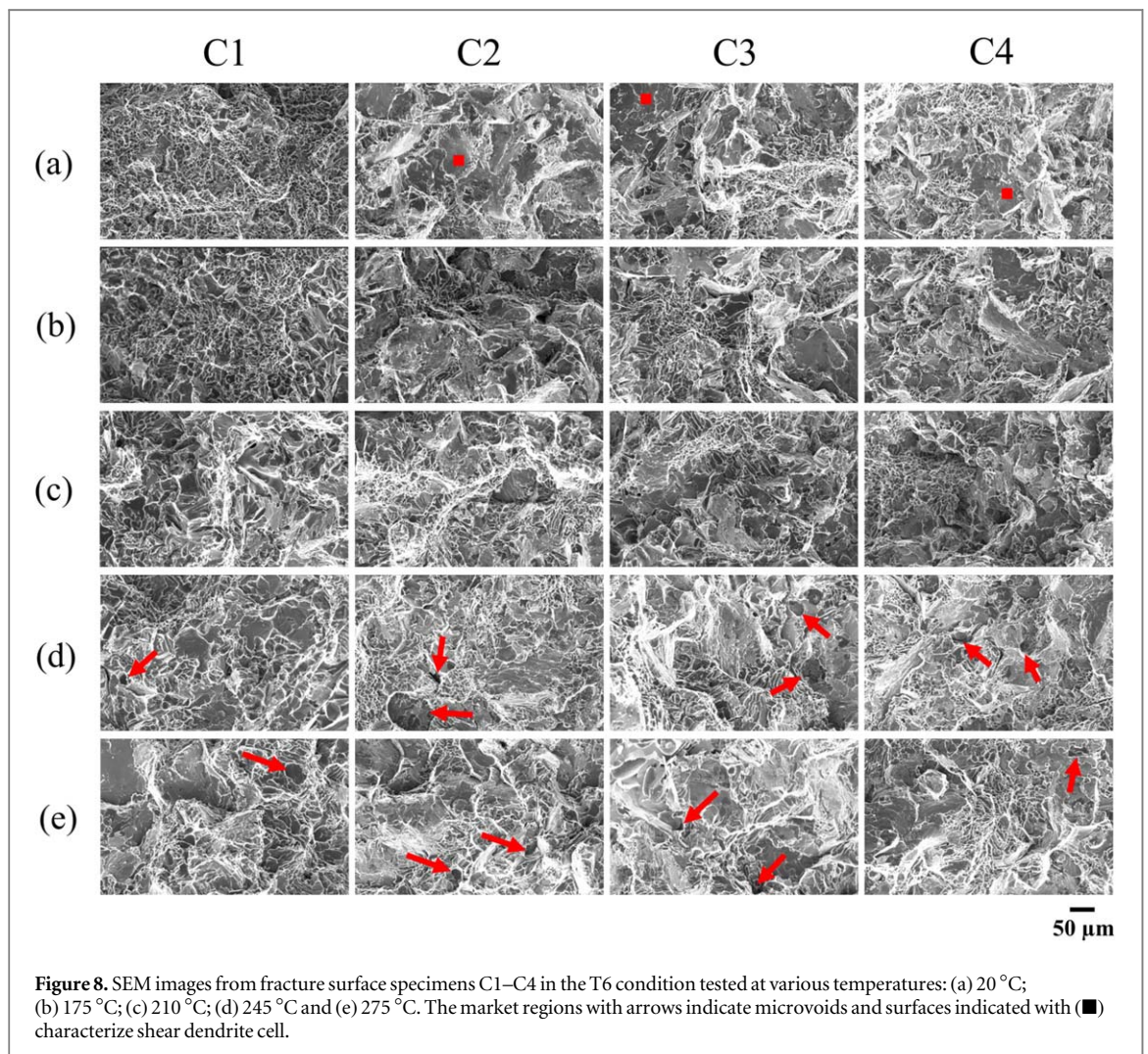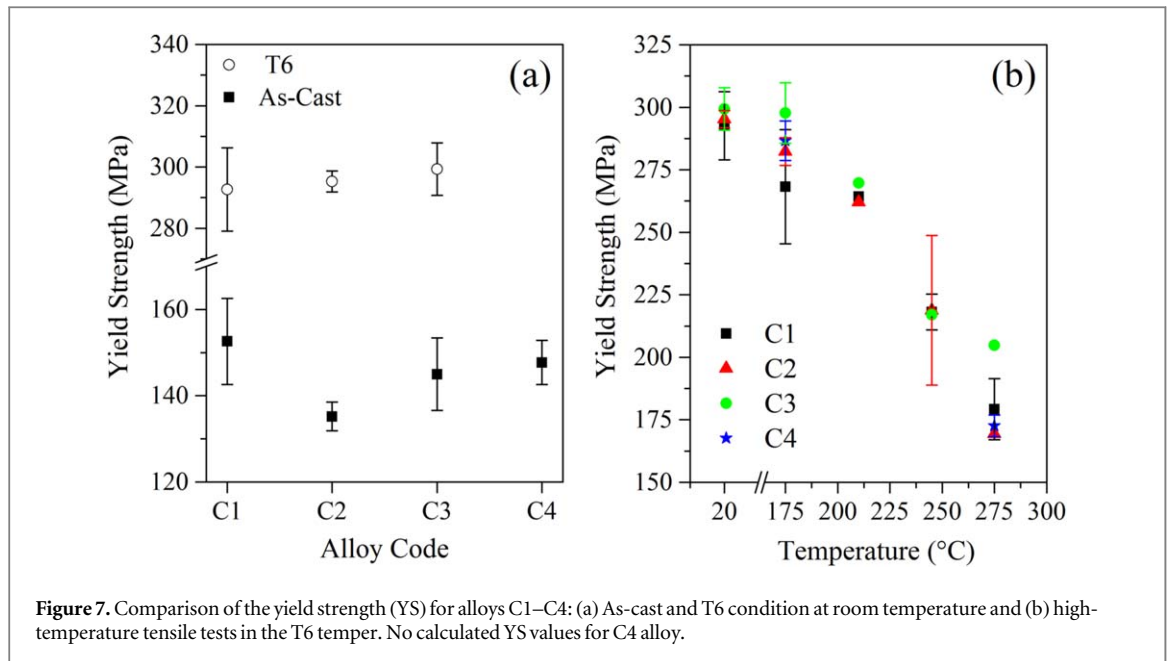
The mechanical properties (YS and UTS) of the alloys evaluated in this work are summarized in table 2. They were further compared to previous works of 3XX.X alloys series from the automotive industry. By analyzing the results obtained by [20], the maximum strength obtained at 190 °C is 290 MPa for Al–Si–Cu–Mg alloy modified with Ni and Zr, while in the present work the findings achieved herein were as a UTS of 284 MPa at 210 °C. Therefore, the Al–Si–Cu–Mg alloy modification by Ce (0.3 wt%) and Zr (0.26 wt%) presents a high potential for high temperature applications.

Figures 7(a) and (b) show the YS for as-cast as well as T6 conditions in tensile tests conducted at 20 °C and high temperatures. For as-cast condition, as can be observed in Figure 7(a), additions of 0.3 wt% Ce + 0.16 wt% Zr (C2 alloy) lead to a reduced yield strength due to the Ce–Cu reaction (intermetallic phases of Ce showed in figures 4(a) and (b)) possibly due to the diminished density of Al$_2$Cu in a matrix formed after solidification. Besides, no meaningful improvements in YS for the as-cast condition at 20 °C were detected, which is in accordance with the literature [5]. Therefore, high levels of YS at 20 °C and age hardened condition of the Al matrix (figure 7(a)) were achieved.

Considering the C4 alloy (0.3 wt% Ce + 0.36 wt% Zr), the YS cannot be calculated by offset method probably due to the drastic reduction of strain by the high content of intermetallic phases formed by Zr. Figure 7(b) shows the reduction of YS of alloys against the temperature due to coarsening of precipitates as already discussed for the high-temperature tensile test (figure 6). The thermal stability of intermetallic phases of Ce and Zr is responsible for slightly improvements in YS of alloy C3 (0.3 wt% Ce + 0.27 wt% Zr), especially at 275 °C (an increase of 13.8%) compared to the base alloy. This Ce–Zr ratio (1:1) showed to be the most efficient combination for keeping the YS at high temperatures.

3.3. Surface fracture

Figure 8 shows the surface fracture for T6 condition in the tensile testing at 20 °C and different temperatures such as 175, 210, 245, and 275 °C. At 20 °C (figure 8(a)), it can be noted small dimples which characterizes the surface fracture of the standard alloy due to the spheroidization of eutectic silicon and a small percentage of intermetallic phases. The spheroidization process is suggested to be the main reason for the good fracture elongation in hardened T6 condition [40], which lead to less stress concentration when compared to acicular Si morphologies [41].

Figure 7. Comparison of the yield strength (YS) for alloys C1–C4: (a) As-cast and T6 condition at room temperature and (b) high-temperature tensile tests in the T6 temper. No calculated YS values for C4 alloy.

Figure 8. SEM images from fracture surface specimens C1–C4 in the T6 condition tested at various temperatures: (a) 20 °C; (b) 175 °C; (c) 210 °C; (d) 245 °C and (e) 275 °C. The market regions with arrows indicate microvoids and surfaces indicated with (■) characterize shear dendrite cell.

For Ce–Zr modified alloys, the coarse network of silicon particles and Ce–Zr intermetallic phases in microstructure raised high levels of stress concentration into the aluminum matrix. The mode of fracture for large dendritic spacing is basic transgranular, according to [42]. This author also comments that in alloys with

larger dendritic spacing dendrite cell, there were localized shear bands generated in the matrix. The shear bands can be seen in surface fracture (indicated as ■) in the test conducted at 20 °C for modified alloys C2, C3 and C4. Some authors [43], studied a cast aluminum alloy with 7% Si and concluded that the fracture path in alloy with large dendrite cell sizes is predominantly transgranular, and for small dendrite cell size, the fracture mode tends to be intergranular. They also commented that the modification of alloys (by Sr addition) shifts the transition in fracture mode towards larger values of the dendrite cell size.

The fracture behavior between 175 °C (figure 8(b)) and 210 °C (figure 8(c)) has shown a mix of brittle cleavage with small areas of plastic deformation for all alloys. For tests at 245 °C (figure 8(d)) and 275 °C (figure 8(e)), the fracture surface of Ce–Zr modified alloy is characterized by the presence of microvoids (marked by arrows) started at 245 °C. These results are similar to the ones obtained in fracture analysis of Al–Si–Cu–Mg alloy with Ni and Zr additions [38]. The authors described that at high temperatures (> 250 °C) the failure mechanism started by voids nucleation near to the intermetallic phases, and Ni and Zr particles are sources of voids and resultant dimples on the fracture surface. Further, they explained that Ni and Zr particles not allowed the development of the progressive cracks, contributing to the increased tensile strength at high temperatures. The fracture of the Al–Si alloy at high temperature is associated with void nucleation and growth according to [44]. The nucleation occurs at the coarse particles and second-phase present in the microstructure. The void nucleation could be the possible explanation for strain reduction of modified alloys at the tensile test performed at 275 °C (figure 6(e)).

4. Conclusions

The effects of Ce and Zr additions on microstructure and mechanical properties of Al–Si–Cu–Mg alloy at room and high temperatures were investigated. The current results can be summarized as follows:

- Both Ce and Zr additions have a high impact on the refinement of the as-cast microstructure. The increase in Zr content improves the refinement effect and the number of intermetallic phases in the aluminum matrix.

- The formation of the Al–Si–Cu–La–Ce intermetallic phase during the solidification of the modified alloys might decrease the amount of available Cu for further precipitation hardening in Alα. This fact leads to a reduction in yield strength.

- For the as-cast condition, the C2 and C3 alloys exhibited similar mechanical behavior when compared to the standard Al–Si–Cu–Mg alloy. However, a combination of 0.3 wt% Ce + 0.36 wt% Zr (C4 alloy) led to a drastic reduction of the mechanical properties (UTS).

- The tensile strength of Ce–Zr modified Al–Si–Cu–Mg alloy decreases with increasing test temperature due to the coarsening of the Cu/Mg precipitates. However, due to the high thermal stability of intermetallic phases in microstructure (Al–Si–Cu–La–Ce and Al–Si–Zr–Ti–Mg) and their interaction with the aluminum matrix during plastic deformation, at 210 °C and 275 °C, the UTS of the C3 alloy (0.3 wt% Ce + 0.27 wt% Zr) increased up to 6.7% and 5.1%, respectively.

- Fracture analyses from the tensile samples showed that Ce and Zr intermetallic particles acted as nucleation points for microvoids, thus decreasing the elongation at temperatures higher than 210 °C.

Acknowledgments

ORCID iDs

William Lemos Bevilaqua ⓘ https://orcid.org/0000-0003-4841-4619
Afonso Reguly ⓘ https://orcid.org/0000-0002-4880-3780

References

[1] Miller W, Zhuang L, Bottema J, Wittebrood A, De Smet P, Haszler A and Vieregge A 2000 Recent development in aluminium alloys for the automotive industry *Mater. Sci. Eng. A* **280** 37–49
[2] Toschi S, Balducci E, Ceschini L, Mørtsell E, Morri A and Di Sabatino M 2019 Effect of Zr addition on overaging and tensile behavior of 2618 aluminum alloy *Metals (Basel).* **9** 130

[3] Kasprzak W, Amirkhiz B S and Niewczas M 2014 Structure and properties of cast Al–Si based alloy with Zr–V–Ti additions and its evaluation of high temperature performance *J. Alloys Compd.* **595** 67–79

[4] Czerwinski F, Shaha S K, Kasprzak W, Friedman J and Chen D L 2016 Aging characteristics of the Al–Si–Cu–Mg cast alloy modified with transition metals Zr, V and Ti *IOP Conf. Ser.: Mater. Sci. Eng.* **117** 012031

[5] Shaha S K, Czerwinski F, Kasprzak W, Friedman J and Chen D L 2015 Microstructure and mechanical properties of Al–Si cast alloy with additions of Zr–V–Ti *Mater. Des.* **83** 801–12

[6] Gao T, Zhu X, Sun Q and Liu X 2013 Morphological evolution of ZrAlSi phase and its impact on the elevated-temperature properties of Al–Si piston alloy *J. Alloys Compd.* **567** 82–8

[7] Govindaraju H K, Jayaraj T, Sadanandarao P R and Venkatesha C S 2010 Evaluation of mechanical properties of as-cast Al–Zn–Ce alloy *Mater. Des.* **31** S24–9

[8] Vončina M, Kores S, Mrvar P and Medved J 2011 Effect of Ce on solidification and mechanical properties of A360 alloy *J. Alloys Compd.* **509** 7349–55

[9] Torre E A D L, Pérez-Bustamante R, Camarillo-Cisneros J, Gómez-Esparza C D, Medrano-Prieto H M and Martínez-Sánchez R 2013 Mechanical properties of the A356 aluminum alloy modified with La/Ce *J. Rare Earths* **31** 811–6

[10] Yang X, Xiong B, Li X, Yan L, Li Z, Zhang Y, Liu H, Yan H and Wen K 2019 Microstructure characterization of as-cast Al–Mg–Si alloys with high content Li element addition *Mater. Res. Express* **6** 1165e5

[11] El-Kady E-S Y, Mahmoud T S and Sayed M A-A 2011 Elevated temperatures tensile characteristics of Cast A356/Al$_3$O$_2$ nanocomposites fabricated using a combination of rheocasting and squeeze casting techniques *Mater. Sci. Appl.* **02** 390–98

[12] Zengin H 2019 Wear and corrosion behavior of multi-walled carbon nanotubes (MWCNTs) reinforced Al-15Mg$_2$Si *in situ* composites *Mater. Res. Express* **6** 1065b8

[13] Shaha S K, Czerwinski F, Kasprzak W, Friedman J and Chen D L 2016 Ageing characteristics and high-temperature tensile properties of Al–Si–Cu–Mg alloys with micro-additions of Cr, Ti, V and Zr *Mater. Sci. Eng. A* **652** 353–64

[14] Toschi S 2018 Optimization of A354 Al–Si–Cu–Mg alloy heat treatment: effect on microstructure, hardness, and tensile properties of peak aged and overaged alloy *Metals (Basel).* **8** 961

[15] Morri A, Ceschini L, Messieri S, Cerri E and Toschi S 2018 Mo Addition to the A354 (Al–Si–Cu–Mg) casting alloy: effects on microstructure and mechanical properties at room and high temperature *Metals (Basel).* **8** 393

[16] Abdelaziz M H, Doty H W, Valtierra S and Samuel F H 2018 Mechanical performance of Zr-containing 354-Type Al–Si–Cu–Mg cast alloy: role of additions and heat treatment *Adv. Mater. Sci. Eng.* **2018** 1–17

[17] Sandoval J H, Mohamed A M A, Valtierra S and Samuel F H 2014 Mechanical performance of a Cast A354 aluminium alloy *Mater. Sci. Forum* **794–796** 489–94

[18] Ceschini L, Morri A, Morri A, Toschi S, Johansson S and Seifeddine S 2015 Effect of microstructure and overaging on the tensile behavior at room and elevated temperature of C355-T6 cast aluminum alloy *Mater. Des.* **83** 626–34

[19] Knipling K E, Dunand D C and Seidman D N 2006 Criteria for developing castable, creep-resistant aluminum-based alloys—A review *Zeitschrift für Metallkunde* **97** 246–65

[20] Hernandez-Sandoval J, Garza-Elizondo G H, Samuel A M, Valtiierra S and Samuel F H 2014 The ambient and high temperature deformation behavior of Al–Si–Cu–Mg alloy with minor Ti, Zr, Ni additions *Mater. Des.* **58** 89–101

[21] Qian H, Zhu D, Hu C and Jiang X 2018 Effects of Zr Additive on Microstructure, Mechanical Properties, and Fractography of Al–Si Alloy *Metals (Basel).* **8** 124

[22] Shaha S K, Czerwinski F, Kasprzak W, Friedman J and Chen D L 2016 Effect of Cr, Ti, V, and Zr micro-additions on microstructure and mechanical properties of the Al–Si–Cu–Mg Cast alloy *Metall. Mater. Trans. A* **47** 2396–409

[23] Chaubey A K, Mohapatra S, Jayasankar K, Pradhan S K, Satpati B, Sahay S S, Mishra B K and Mukherjee P S 2009 Effect of cerium addition on microstructure and mechanical properties of Al–Zn–Mg–Cu alloy *Trans. Indian Inst. Met.* **62** 539–43

[24] Cerija D, Zlitini L, Kores S, Von M, Kosec B, Mrvar P and Medved J 2010 Effect Of Cerium Additions On The AlSi17 Casting Alloy *Materials and Technology* **44** 137–40

[25] Vončina M, Medved J, Bončina T and Zupanič F 2014 Effect of Ce on morphology of α(Al)–Al$_2$Cu eutectic in Al–Si–Cu alloy *Trans. Nonferrous Met. Soc. China* **24** 36–41

[26] Wang W T, Zhang X M, Gao Z G, Jia Y Z, Ye L Y, Zheng D W and Liu L 2010 Influences of Ce addition on the microstructures and mechanical properties of 2519A aluminum alloy plate *J. Alloys Compd.* **491** 366–71

[27] Ye L, Gu G, Liu J, Jiang H and Zhang X 2013 Influence of Ce addition on impact properties and microstructures of 2519A aluminum alloy *Mater. Sci. Eng. A* **582** 84–90

[28] Sims Z C *et al* 2017 High performance aluminum–cerium alloys for high-temperature applications *Mater. Horizons.* **4** 1070–8

[29] Voort G F V 1999 *Metallography: Principles and Practice* (United States of America: ASM International) p 752

[30] Wang F, Qiu D, Liu Z L, Taylor J A, Easton M A and Zhang M X 2013 The grain refinement mechanism of cast aluminium by zirconium *Acta Mater.* **61** 5636–45

[31] Baradarani B and Raiszadeh R 2011 Precipitation hardening of cast Zr-containing A356 aluminium alloy *Mater. Des.* **32** 935–40

[32] Dang J Z, Huang Y F and Cheng J 2009 Effect of Sc and Zr on microstructures and mechanical properties of as-cast Al–Mg–Si–Mn alloys *Trans. Nonferrous Met. Soc. China (English Ed.* **19** 540–4

[33] Okamoto H 2011 Al–Ce (Aluminum-Cerium) *J. Phase Equilibria Diffus.* **32** 392–3

[34] Murray J, Peruzzi A and Abriata J P 1992 The Al–Zr (aluminum-zirconium) system *J. Phase Equilibria.* **13** 277–91

[35] Lados D A, Apelian D and Wang L 2010 Solution treatment effects on microstructure and mechanical properties of Al-(1 to 13 pct)Si–Mg cast alloys *Metall. Mater. Trans. B* **42** 171–80

[36] Sepehrband P, Mahmudi R and Khomamizadeh F 2005 Effect of Zr addition on the aging behavior of A319 aluminum cast alloy *Scr. Mater.* **52** 253–7

[37] Xinxiang Y, Dengfeng Y and Zhiming Y 2016 Effects of cerium and zirconium microalloying addition on the microstructures and tensile properties of novel Al–Cu–Li alloys *Rare Met. Mater. Eng.* **45** 1917–23

[38] Mohamed A M A, Samuel F H and Kahtani S A 2013 Microstructure, tensile properties and fracture behavior of high temperature Al–Si–Mg–Cu cast alloys *Mater. Sci. Eng. A* **577** 64–72

[39] Elhadari H A, Patel H A, Chen D L and Kasprzak W 2011 Tensile and fatigue properties of a cast aluminum alloy with Ti, Zr and V additions *Mater. Sci. Eng. A* **528** 8128–38

[40] Ogris E, Wahlen A, Lüchinger H and Uggowitzer P 2002 On the silicon spheroidization in Al–Si alloys *J. Light Met.* **2** 263–9

[41] Suarez M A, Figueroa I, Cruz A, Hernandez A and Chavez J F 2012 Study of the Al-Si-X system by different cooling rates and heat treatment *Mater. Res.* **15** 763–9

[42] Wang Q G 2003 Microstructural effects on the tensile and fracture behavior of aluminum casting alloys A356/357 *Metall. Mater. Trans. A* **34** 2887–99

[43] Wang Q G, Cáceres C H and Griffiths J R 1997 Transgranular and intergranular fracture in Al–Si–Mg casting alloys *International Conference on Fracture (Sydney, 1997)* 2511–18

[44] Rajaram G, Kumaran S and Rao T S 2010 High temperature tensile and wear behaviour of aluminum silicon alloy *Mater. Sci. Eng. A* **528** 247–53